ACTA IMEKO
ISSN: 2221-870X
June 2025, Volume 14, Number 2, 1 - 8

Switching linear parameter varying control for a robotic manipulator

Zoltán Téczely[1], Bálint Kiss[1]

[1] *Department of Control Engineering and Information Technology, Budapest University of Technology and Economics, 2, Magyar Tudósok Körútja, Budapest, Hungary*

ABSTRACT
This paper introduces a synthesis study of a switching Linear Parameter Varying (LPV) controller with multiple polytopic subregions, considering separate parameter-dependent Lyapunov functions. The parameter space setup is designed with overlapping subregions in which safe controller switching is ensured by hysteresis switching logic. Robotic manipulators, like any mechatronic systems, are burdened with unmodelled characteristics such as friction phenomena and actuator dynamics, as well as nonlinear dynamics. These effects might be countered by LPV controllers, although they may be too conservative for production. The switching controller can decrease conservatism utilising separate Lyapunov functions while maintaining essential features of a general H_∞ LPV controller, such as global asymptotic stability over the entire parameter space. The suggested method is applied on a real-life 2-DOF SCARA-type robotic manipulator, and extensive testing results are presented along with some of the key challenges that arise when the application is moved from simulation to real-life. Primary considerations with respect to the application of switching control are studied in detail, including the number and shape of subregions, overlapping percentage, switching surface orientation, and scheduling parameter selection.

Section: RESEARCH PAPER

Keywords: LPV; polytopic; robotic arm; switched systems; Lyapunov theory; LMI

Citation: Z. Téczely, B. Kiss, Switching linear parameter varying control for a robotic manipulator, Acta IMEKO, vol. 14 (2025) no. 2, pp. 1-8. DOI: 10.21014/actaimeko.v14i2.1741

Section Editor: Leonardo Iannucci, Politecnico di Torino, Italy

Received January 5, 2024; **In final form** April 24, 2025; **Published** June 2025

Corresponding author: Zoltán Téczely, e-mail: zoltan.teczely@iit.bme.hu

1. INTRODUCTION

Polytopic Linear Parameter Varying (LPV) control has seen great popularity in the past decades and continues to be an essential tool in the nonlinear control palette. Part of its charm among researchers and practitioners alike is its relative ease of use, stemming from the fact that LPV can be traced back to well-understood LTI and LTV methodologies. Although heavily relying on linear methods, the LPV system class can be efficiently used to describe essentially nonlinear systems or alternatively, to account for uncertain parameters in linear models. For general LPV control systems, a strong set of results is available, most prominently quadratic stability can be guaranteed over the entire parameter region if it is maintained at the polytope vertices.

The foundations of the mathematical toolset and basic ideas of LPV control paired with Linear Matrix Inequalities (LMIs) were laid in [1] and [2] in the early 90s, while [3] extended basics with multi-objective control criteria. Providing a general overview of the available methods, [4] presented a milestone work but lacked the polytopic approach.

Robotic arm control has been intensively studied in the past decades and there is no shortage of LPV based control schemes. A standard LPV H_∞ approach is presented in [5] while controller conservatism reduction is covered in [6] and [7]. Further remarkable results include but are not limited to [8], [9]. Despite extensive research works, there is still an ongoing interest in improving controller performance in robotics, especially due to the conservative nature of robust control methods. LPV control structures simultaneously address robust behaviour and solid performance, but controller conservatism remains a solvable problem, together with robustness issues due to unmodelled behaviour such as friction phenomena, backlash and neglected actuator dynamics. In the XXIst century, conservatism reduction has been a primary driving force for development while maintaining the requirement for robust stability. The main directions of research were the reduction of the parameter space e.g. [6], [10], and the introduction of parameter-dependent Lyapunov functions [11], [12].

In more recent studies, the new subclass of switched LPV systems has evolved in which a common Lyapunov function is no longer a necessity allowing for higher performance [13]-[16].

To ensure safe switching on subregion boundaries, the most common strategies are hysteresis switching [13], in which a dead-zone is defined and switching may take place on different boundary layers depending on the evolution of the parameter vector, and average dwell time-based switching logic, which prevents chattering on the boundaries by predefining a dwell time during which only one switch may occur. Recall that although switching is more often employed as part of fault tolerant control strategies, an increasing number of LPV switching control applications are emerging especially from the aerospace industry [17]-[19]. The requirement of smooth switching and chattering avoidance drives the need for more complicated controllers such that the previously mentioned robust stability and performance is maintained.

On the other hand, methods for systematic subdivision of the parameter space are less common with the notable exception of [20]. The heuristic nature of the subdivision of the parameter space has been addressed by the authors in [21] where a systematic subregion layout selection was proposed based on optimization techniques.

The primary contribution of this paper is the application of switching LPV control with hysteresis switching logic on a two degrees-of-freedom (2-DOF) robotic arm located at the Robotics Laboratory at the Budapest University of Technology and Economics. This extends the list of available LPV-related options bringing about a significant performance improvement. On top of implementing the set of LPV controllers, several parameter subregion layouts are tested, and the method is evaluated numerically on a real-life robot covering a series of operation scenarios.

The remainder of the paper is organized as follows. The next section gives an in-depth introduction to the robotic arm system. Section 3 introduces the notion of switched LPV systems, while Section 4 presents the controller synthesis framework. Section 5 includes the specific challenges characteristic of robotic arms together with test implementation and numerical results. Finally, Section 6 concludes the paper and gives suggestions for further studies.

2. ROBOT MODELLING

The robotic arm is characterized by arm lengths (l_1, l_2), distances to the centre of gravities $(l_{c,1}, l_{c,2})$, arm weights (m_1, m_2), inertias (J_1, J_2) and joint angles (q_1, q_2), corresponding to the first and second link, respectively. With these, the schematic view of the robot is presented in Figure 1.

By introducing shorthand notations $C_1 = \cos(q_1)$, $S_1 = \sin(q_1)$, $C_{12} = \cos(q_1 + q_2)$ and $S_{12} = \sin(q_1 + q_2)$ the positions of the centre of gravity of the links read

$$r_1 = \begin{bmatrix} l_{c,1} C_1 \\ l_{c,1} S_1 \end{bmatrix}, \qquad r_2 = \begin{bmatrix} l_1 C_1 + l_{c,2} C_{12} \\ l_1 S_1 + l_{c,2} S_{12} \end{bmatrix}. \tag{1}$$

Hence velocities are derived as

$$v_1 = \begin{bmatrix} -l_{c,1} \dot{q}_1 S_1 \\ l_{c,1} \dot{q}_1 C_1 \end{bmatrix}, \tag{2}$$

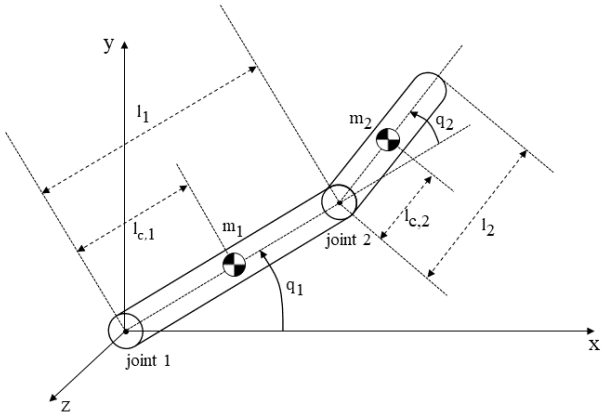

Figure 1. Schematic representation of the 2-DOF robotic arm.

$$v_2 = \begin{bmatrix} -l_1 \dot{q}_1 S_1 - l_{c,2}(\dot{q}_1 + \dot{q}_2) S_{12} \\ l_1 \dot{q}_1 C_1 - l_{c,2}(\dot{q}_1 + \dot{q}_2) C_{12} \end{bmatrix}.$$

The standard model of a robotic arm can be derived with the Lagrangian approach starting from

$$L(q, \dot{q}) = K(q, \dot{q}) - P(q). \tag{3}$$

where

$$K(q, \dot{q}) = \frac{1}{2}(m_1 v_1^T v_1 + m_2 v_2^T v_2 + J_1 \dot{q}_1^2 + J_2 (\dot{q}_1 + \dot{q}_2)^2)$$

is the kinetic energy and $P(q)$ is the potential energy of the system. The present paper only deals with motions on a horizontal plane, therefore no gravity-related terms appear yielding: $P(q) = 0$. With that, the Euler-Lagrange equations take the form

$$H(q)\ddot{q} + h(q, \dot{q}) = \tau, \tag{4}$$

where $\tau \in \mathbb{R}^2$ is the vector of joint torques, the matrix H contains the inertial terms, the matrix h includes centrifugal and Coriolis-effect related terms. The elements of the matrices are

$$\begin{aligned} H_{11}(q) &= m_1 l_{c,1}^2 + m_2 \left(l_1^2 + l_{c,2}^2 + 2 l_1 l_{c,2} C_2\right) + J_1 + J_2 \\ H_{12}(q) &= H_{21}(q) = m_2 \left(l_1 C_2 + l_{c,2}\right) l_{c,2} + J_2 \\ H_{22}(q) &= m_2 l_{c,2}^2 + J_2 \\ h_1(q, \dot{q}) &= -S_2 \dot{q}_2 m_2 l_{c,2} l_1 (2\dot{q}_1 + \dot{q}_2) \\ h_2(q, \dot{q}) &= S_2 m_2 l_{c,2} l_1 \dot{q}_2^2 . \end{aligned} \tag{5}$$

Since $H(q)$ is positive definite, its inverse also exists, thus the model can be easily rewritten into state-space form with an additional pair of integrators.

The model is further modified to include friction terms. Friction is modelled as a combination of viscous and Coulomb parts. Asymmetric viscous friction can be described by

$$\tau_{v,i} = \begin{cases} b_i^+ \dot{q}_i & if\ sign(\dot{q}_i) > 0 \\ b_i^- \dot{q}_i & if\ sign(\dot{q}_i) < 0 , \end{cases} \tag{6}$$

where b_i^+ and b_i^- are the viscous friction coefficients for the positive and negative movement direction, respectively, for the i^{th} link. The resulting state-space representation is thus

$$\begin{bmatrix}\dot{q}\\ \ddot{q}\end{bmatrix}=\begin{bmatrix}0 & I\\ 0 & -H(q)^{-1}\left(h(q,\dot{q})+\begin{bmatrix}\tau_{v,1}\\ \tau_{v,2}\end{bmatrix}\right)\end{bmatrix}\begin{bmatrix}q\\ \dot{q}\end{bmatrix}+\begin{bmatrix}0\\ H(q)^{-1}\end{bmatrix}\begin{bmatrix}\tau_1\\ \tau_2\end{bmatrix}. \quad (7)$$

Viscous friction can be directly included in the linearized model, but the Coulomb part is included in the control scheme as a feedforward element

$$\tau_{C,i}=\begin{cases}c_i^{+}\text{sign}(\dot{q}_i) & if\ \text{sign}(\dot{q}_i)>0\\ c_i^{-}\text{sign}(\dot{q}_i) & if\ \text{sign}(\dot{q}_i)<0\,,\end{cases} \quad (8)$$

where c_i^{+} and c_i^{-} are the Coulomb coefficients for positive and negative rotational direction, respectively. For the actual robotic arm used in this paper, the exact parameters are acquired based on [22]. Asymmetry of the identified parameters might be a result of gear toothing, slightly imperfect placement of the pivots even actuator character. This way, the real-life robotic manipulator necessitates a 2-DOF control structure with a feedforward term represented by Coulomb friction and the switching LPV feedback gain described in more detail.

3. SWITCHED LINEAR PARAMETER VARYING SYSTEMS

3.1. LPV description

Consider a standard LPV system described by

$$P(\varphi)=\begin{bmatrix}A(\varphi) & B_1(\varphi) & B_2(\varphi)\\ C_1(\varphi) & D_{11}(\varphi) & D_{12}(\varphi)\\ C_2(\varphi) & D_{21}(\varphi) & D_{22}(\varphi)\end{bmatrix}. \quad (9)$$

It is assumed that the parameter vector φ and its derivative are bounded and are located in the hypercubes

$$S_\varphi := \left\{(\varphi_1,\dots,\varphi_p)^T : \varphi_j \in \left[\underline{\varphi_j},\overline{\varphi_j}\right], j\in\mathcal{J}_p\right\} \quad (10)$$

$$S_v := \left\{(v_1,\dots,v_p)^T :\ v_j \in \left[\underline{v_j},\overline{v_j}\right],\ \ j\in\mathcal{J}_p\right\} \quad (11)$$

respectively, and the values of the scheduling parameter vectors are available in real time. By taking all possible permutations of the bounds of the parameters, $N=2^p$ number of vectors ω_i are formed such that the parameter vector admits the polytopic form

$$\varphi\in Co\{\omega_1\dots\omega_N\} := \left\{\sum_{i=1}^{N}\mu_i\,\omega_i :\ \mu_i\geq 0,\quad \sum_{i=1}^{N}\mu_i=1\right\}, \quad (12)$$

where every combination will lie inside the convex hull (Co) of vertices and any intermediate parameter values can be formed by the convex combination of the vertex parameters. In turn, if the dependence of $P(\varphi)$ on the scheduling variables is affine, all possible models will lie in the convex hull of models $\wp$ whose vertices are the images of the vertices ω_i

$$\wp := Co\{P_1\dots P_N\} := \left\{\sum_{i=1}^{N}\mu_i\,P_i :\ \mu_i\geq 0,\quad \sum_{i=1}^{N}\mu_i=1\right\}, \quad (13)$$

where $\wp$ is defined as the convex hull of vertex models located at the vertices of the polytope and μ_i are weighting functions written compactly as

$$\mu_i(\varphi)=\frac{\prod_{i=1}^{2^p}\left|\varphi_j-\text{compl}(\text{coin}\,\varphi_i)_j\right|}{\prod_{j=1}^{p}(\overline{\varphi_j}-\underline{\varphi_j})}. \quad (14)$$

Here, p is the number of scheduling variables, $N=2^p$ is the number of polytope vertices, $\underline{\varphi_j}$ and $\overline{\varphi_j}$ are the lower and upper bounds of the parameters respectively, and $\text{compl}(\text{coin}\,\varphi_i)_j$ denotes the complementary of φ_i which is the i^{th} vertex of the polytope. Graphically, this means that each vertex has a weight between the extremum models on that vertex according to the current value of the corresponding scheduling parameter.

With (13) and (14) a polytopic formulation of the LPV system (9) can be constructed with the sector nonlinearity approach [23], [24] even if the matrices are nonlinear functions of the scheduling variables.

As an alternative, in the case of the 2-DOF robotic arm, we select $\cos(q_2)$ and $\sin(q_2)\dot{q}_2$ as preliminary scheduling variables. We require that they be available in real time and explicitly define each element of the state-space matrices of the model. After the reformulation into state-space format, these parameters no longer enter the matrices in a linear fashion due to matrix inversion in (7) therefore the nonconstant elements of the matrices A and B must be considered as true scheduling variables. In practice, this can lead to up to 8 scheduling parameters and indeed, every nonconstant element is scheduled by varying parameters, resulting in increased design complexity and critical conservatism. One way of relaxing this burden is by performing sensitivity analysis from variations in the preliminary scheduling variables to variations in the matrices and keeping only the elements most exposed. This can be regarded as a similar but more straightforward and easily applicable procedure as described in [6].

For LPV controller design description, it is necessary to make the following assumptions for the plant:

(A1) $D_{22}(\varphi)=0$.

(A2) $[B_2^T(\varphi)\ D_{12}^T(\varphi)]$ and $[C_2(\varphi)\ D_{21}(\varphi)]$ have full row ranks for all φ.

(A3) The set of matrices $\left(A(\varphi),B_2(\varphi),C_2(\varphi)\right)$ is parameter-dependent, stabilizable, and detectable for all φ.

3.2. Switched LPV systems

Let us now consider the case when the full polytope consists of a finite number of closed subsets $\wp=\bigcup\wp_i\,,\quad i\in Z_N$ where $Z_N=\{1,2,\dots,N\}$. This setup can be described by a family of switching surfaces S_{ij} in the parameter space S_φ and the neighbouring parameter subsets have overlapping regions or are completely disjoint. In this paper, the case with overlapping subsets is considered.

3.3. Controller design

Problem formulation:

Design a family of state-feedback LPV controllers

$$u=F_{k,i}(\varphi)x,\quad i\in Z_N \quad (15)$$

each suitable for a specific subregion $\wp_i$ with guaranteed quadratic stability over the entire operating region $\wp$ with H_∞ performance. Moreover, safe switching between adjacent controllers shall be ensured by an appropriate logic guaranteeing

stability of the closed-loop system when the state trajectories hit the switching surface S_{ij} by adopting separate Lyapunov functions for the individual LPV subregions. It is to be noted, that the discontinuous Lyapunov function (henceforth denoted as $V_\sigma(x_{CL}, \varphi)$) does not need to be decreasing through the entire parameter trajectory. Rather, it is sufficient to require that it decreases in the active parameter region, given that an appropriate switching logic is adopted [13].

Switching evolution:

The switching between adjacent LPV controllers occurs when the parameters hit the switching surfaces S_{ij}. To formulate switching as a triggered event, the introduction of a switching signal σ is necessary. It is defined as a piecewise constant function and is assumed to be continuous from the right everywhere. For the general LPV system (9) and the switching state-feedback control law (15) the closed-loop system is described as

$$\begin{bmatrix} \dot{x}_{CL} \\ e \end{bmatrix} = \begin{bmatrix} A(\varphi) + B_2(\varphi)F_\sigma(\varphi) & B_1(\varphi) \\ C_1(\varphi) + D_{12}(\varphi)F_\sigma(\varphi) & D_{11}(\varphi) \end{bmatrix} \begin{bmatrix} x_{CL} \\ d \end{bmatrix}, \tag{16}$$

where the index σ indicates switching design.

4. SWITCHING H_∞ CONTROL

4.1. LPV H_∞ control

Typically, robust controller synthesis can be performed in a tractable manner with LMI formulation [25]. A robust stability guarantee is held by virtue of the well-known Bounded Real Lemma (BRL). It can also be shown that this property still stands for LPV systems as long as the scheduling variables enter the matrices in a linear fashion [1], [2]. Although analytical solutions for the dynamic output feedback case do exist [14], they are formulated in a nonconvex way and the numerical problem is not solvable in polynomial time, i.e. numerical solvers are generally not tractable. Since, in the case of the robotic manipulator, measurements are available for every state, we resort to the state-feedback case.

4.2. Switching control with parameter-dependent Lyapunov functions

Let us suppose that there exist a family of positive definite matrix functions $\{X_i(\varphi)\}_{i\in Z_N}$ that are smooth over their corresponding parameter subset $\wp_i$. For each subset, parameter-dependent Lyapunov functions can be defined and collected into a family of Lyapunov functions as

$$V_\sigma(x_{CL}, \varphi) = x_{CL}^T X_\sigma(\varphi) x_{CL}\,, \tag{17}$$

where the value of the switching signal selects the active operating region $\wp_i$ and determines the corresponding matrix function $X_i(\varphi)$. Since the active controller can be regarded as an individual LPV control law, the guarantee for stability can be given by adopting the correct switching logic alone [13], [14], further restrictions on the separate subregions are not needed. This leads to relaxed constraints over the LMI optimization procedure ultimately resulting in a less conservative controller design.

4.3. Hysteresis switching

As opposed to dwell time-based switching strategies, hysteresis switching assumes an overlapping region between any pair of adjacent parameter subsets resulting in two switching surfaces for a pair of subregions. Hysteresis and switching surfaces corresponding to oriented controller switching are presented in Figure 2, for the case of two scheduling variables such that only the first dimension of the parameter space is subdivided.

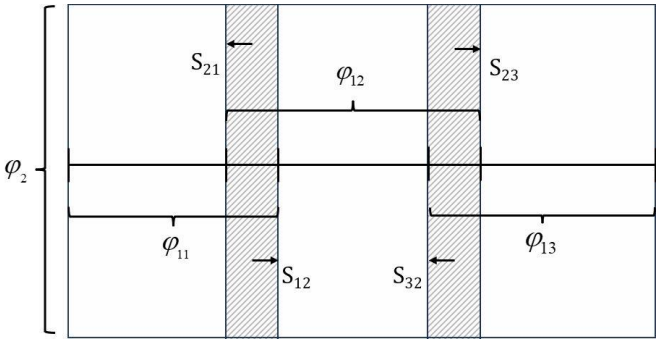

Figure 2. Subdivided parameter space with 3 overlapping subregions and hysteresis logic. Example presented with 2 scheduling variables.

The one-directional move from subregion $\wp_i$ to subregion $\wp_j$ is denoted by S_{ij}. Switching is performed whenever the parameter trajectory hits any of the switching surfaces. The switching rule described in time as a function of σ is as follows:

Algorithm 1

Input: scheduling parameter vector φ
Output: Switching signal σ

Let $\sigma(0) = i \quad if \quad \varphi \in \wp_i$
for $t > 0$
  if $\sigma(t^-) = i$ *and* $\varphi \in \wp_i$
    $\sigma(t) = i$
  if $\sigma(t^-) = i$ *and* $\varphi \in \wp_j - \wp_i$
    $\sigma(t) = j$
  end
end

For the stable operation of the switching LPV closed-loop system (16) the general requirements are as follows: Firstly, the operation of each LPV controller corresponding to the individual subregions $\wp_i$ must comply with classical polytopic LPV criteria, that is, the fulfilment of the BRL is a necessary condition. Secondly, switching logic must be defined according to necessary and sufficient stability conditions, which means the disruption introduced by the switching event must be accounted for by the switching rule itself. The following two points formalize these requirements.

Corollary 1 (Bounded Real Lemma for each LPV subsystems):

The following statements are equivalent:

1. The LPV system G_i has H_∞ performance with γ_i: $\|G_i\|_{H\infty} \le \gamma_i$
2. There exist positive definite matrices $X_i \succ 0$, such that

$$\begin{bmatrix} \left\{ \begin{matrix} A_i(\varphi)^T X_i(\varphi) + X_i(\varphi) A_i(\varphi) \\ -\sum_{k=1}^{N} \{\underline{v_k}, \overline{v_k}\} \frac{\partial X_i}{\partial \varphi_k} \end{matrix} \right\} & * & * \\ B_i(\varphi)^T X_i(\varphi) & -\gamma_i I & * \\ C_i(\varphi) & D_i(\varphi) & -\gamma_i I \end{bmatrix} \prec 0 \tag{18}$$

3. The LMI (18) is feasible if and only if the corresponding Algebraic Riccati Inequality has a real solution $X_i(\varphi) = X_i(\varphi)^T$:

$$A_i{}^T X_i + X_i A_i + C_i{}^T C_i + \left(X_i B_i + C_i{}^T D_i\right)\left(I - D_i{}^T D_i\right)^{-1}\left(X_i B_i + C_i{}^T D_i\right)^T \prec 0 \tag{19}$$

where the dependences $X_i(\varphi), A_i(\varphi), B_i(\varphi), C_i(\varphi)$ and $D_i(\varphi)$ are absent for conciseness and $*$ denotes matrix elements that can be deduced by symmetry.

The matrix function $X_i(\varphi)$ is related to the Lyapunov function of the closed-loop system when the i^{th} controller is active. For safe switching, we must require, that when the parameter trajectory hits the switching surface S_{ij} the value of the Lyapunov function corresponding to the subregion currently under activation is always less than or equal to the value of the Lyapunov function of the previous subregion, in other words, the Lyapunov function is always non-increasing at switching events, that is:

Corollary 2 (Safe switching requirement)

$$X_i(\varphi) \geq X_j(\varphi) \tag{20}$$

yielding $V_i(x_{CL}, \varphi) \geq V_j(x_{CL}, \varphi)$ eventually allowing safe activation of the j^{th} controller set [14].

By the combination of the two previous statements and applying the synthesis technique of [1], necessary and sufficient conditions for switching LPV controller synthesis can be formed:

Corollary 3 (Switching LPV synthesis conditions):

According to [13], [14] the closed-loop LPV system (16) is exponentially stabilized by state-feedback switching LPV controllers over the entire parameter region $\wp$ and the $\mathcal{L}_2$ norm mapping d to e is bounded by $\gamma = \max\{\gamma_i\}_{i \in Z_N}$, that is, $\|e\|_2 \leq \gamma \|d\|_2$ performance is reached if there exist positive-definite matrix functions $R_i(\varphi)$ such that for any $\varphi \in \wp_i$,

$$\mathcal{N}_R^T \begin{bmatrix} \left\{ \begin{matrix} R_i A^T + A R_i \\ -\sum_{k=1}^{N} \{\underline{v_k}, \overline{v_k}\} \frac{\partial R_i}{\partial \varphi_k} \end{matrix} \right\} & R_i C_1^T & B_1 \\ C_1 R_i & -\gamma_i I & D_{11} \\ B_1^T & D_{11}^T & -\gamma_i I \end{bmatrix} \mathcal{N}_R \prec 0 \tag{21}$$

where $\mathcal{N}_R = Ker[B_2^T \quad D_{12}^T \quad 0]$ is the orthogonal complement and $\underline{v_k}$ and $\overline{v_k}$ are the lower and upper bounds of the derivatives of the parameters respectively. The dependences $A(\varphi), B(\varphi), C(\varphi)$ and $D(\varphi)$ on the parameters are omitted for conciseness. The matrices R_i are defined to be linear and parameter-dependent, that is, they have the form $R_i(\varphi) = R_i^0 + R_i^1 \varphi$.

It is also required, that for any $\varphi \in S_{ij}$, that is when the parameter trajectory is hitting the switching surface,

$$R_i \leq R_j. \tag{22}$$

Finally, the switching LPV feedback gains can be calculated as:

$$F_i = -(D_{12}^T D_{12})^{-1}[\gamma_i B_2^T R_i^{-1} + D_{12}^T C_1] \tag{23}$$

for any $i \in Z_N$.

Proof: The proof can be found in [14].

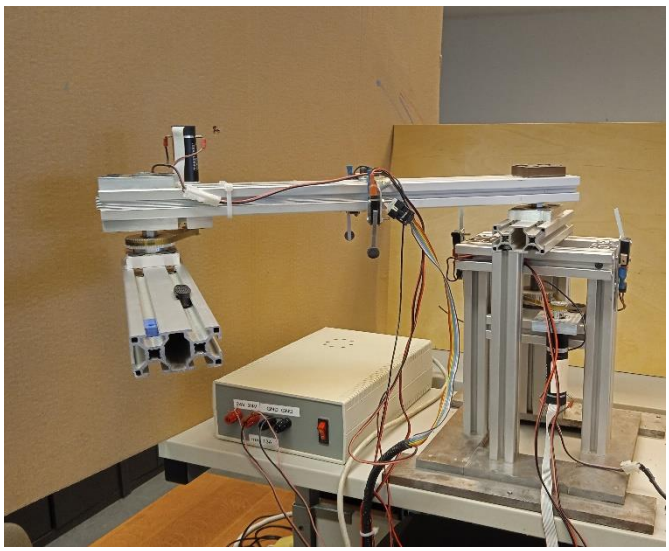

Figure 3. 2-DOF robotic arm system under test.

5. RESULTS

This section is to present the results acquired from the actual 2-DOF robotic arm located at BME Robotics Laboratory, Figure 3. The parameters of the system are the same as described in [26]. For LMI formulation LMI Lab [27] was used. Tests were run on a custom-built robot with two Maxon DC motors and Quarc real-time kernel. Non-modelled factors and known deviations from the system model include actuator dynamics, friction, backlash, and the misalignment of the normal vector to the robot's motion plane with the vertical direction. Out of these, geometric imperfections and actuator dynamics are negligible within good reason. Deviation from horizontal placement did not result in drifting movement from any initial position when out of operation, which means, the static friction in both directions is higher than the effect of geometric tilts. Actuator dynamics were not considered because the dynamical range of the motors are well within the intended operation for the specific application, that is, the performance of the motor starts to degrade at an operating point outside the expected operating range of the manipulator.

Three main considerations were made for the controller design and the test series were defined accordingly. Firstly, the number and layout of the parameter subregions was considered then the parameter along which switching took place was varied. Since parameter space subdivision induces an exponential growth in the number of subregions, the number of LMIs to be solved also grows. For this reason, only cases wherein switching can occur along a single dimension were tested. Finally, a standard polytopic LPV layout was included as a reference.

Parameter values of the model (5) are based on [28]. It is assumed that the velocities cannot surpass 3 rad/s in either direction and both segments make full rotations. Varying preliminary parameters $\cos(q_2)$ and $\sin(q_2)\dot{q}_2$ between these presumed limits yields a set of variations in the elements of the matrices A and B. Since all elements of the matrices are multiplied by velocity type states, all are weighted equally. Finally, elements A_{44} and B_{42} proved to be most sensitive to variations in the preliminary scheduling variables. Their respective bounds were set as $[-5.3 \quad 5.3]$ and $[96 \quad 125]$ for the standard polytopic LPV controller used as a reference.

Table 1. Scheduling variable switching layouts corresponding to state-space matrices.

$A_{44,1}$	$A_{44,2}$	$A_{44,3}$	$B_{42,1}$	$B_{42,2}$
[−5.3 1]	[−1 5.3]	-	[96 125]	-
[−5.3 0.1]	[−0.1 5.3]	-	[96 125]	-
[−5.3 −1]	[−1.5 1.5]	[1 5.3]	[96 125]	-
[−5.3 5.3]	-	-	[96 106]	[105 125]

For switching control, the subregion boundary setups are collected in Table 1.

The best performing results could be achieved by the following LPV layout:

$$A_{1,\min} = \begin{bmatrix} 0_{2x2} & I_{2x2} \\ 0_{2x2} & \begin{bmatrix} 0 & 0 \\ 0 & -5.3 \end{bmatrix} \end{bmatrix}, A_{1,\max} = \begin{bmatrix} 0_{2x2} & I_{2x2} \\ 0_{2x2} & \begin{bmatrix} 0 & 0 \\ 0 & 1 \end{bmatrix} \end{bmatrix},$$

$$A_{2,\min} = \begin{bmatrix} 0_{2x2} & I_{2x2} \\ 0_{2x2} & \begin{bmatrix} 0 & 0 \\ 0 & -1 \end{bmatrix} \end{bmatrix}, A_{2,\max} = \begin{bmatrix} 0_{2x2} & I_{2x2} \\ 0_{2x2} & \begin{bmatrix} 0 & 0 \\ 0 & 5.3 \end{bmatrix} \end{bmatrix},$$

$$B_{\min} = \begin{bmatrix} 0_{2x2} \\ \begin{bmatrix} 0 & 0 \\ -10 & 96 \end{bmatrix} \end{bmatrix}, B_{\max} = \begin{bmatrix} 0_{2x2} \\ \begin{bmatrix} 0 & 0 \\ -10 & 125 \end{bmatrix} \end{bmatrix}.$$

Building on the defined LPV layout, controller synthesis was done by solving (21) and (22) for both subregions for which the matrices R_i have the form $R_i(\varphi) = R_i^0 + R_i^1\varphi$. Once the convex LMI problem has been solved, the controller could be recovered by (24). Static weights for performance (W_e), actuator effort (W_u) and disturbance rejection (W_d) were set for both subregions. Since the best layout came out to be symmetrical, static weight tuning turned out to be identical for the two subregions:

$$W_{u1} = 250, \quad W_{u2} = 250,$$

$$W_{e1} = 100000, \quad W_{e2} = 100000,$$

$$W_{d1} = 1000, \quad W_{d2} = 2000.$$

Besides the switching LPV controller, a feedforward part was also added due to high static friction levels. Although identification was previously performed based on a Coulomb model, the latest reconstruction on the robot resulted in altered parameters, therefore friction parameters had to be acquired heuristically. The general controller structure is presented in Figure 4.

Test cases were designed to cover the entire operating region and to pass switching surfaces in a variety of frequencies and directions. These test cases include a circular chirp trajectory and multiple step references to mimic point-to-point (P2P) motions.

Figure 5 presents a series of circular reference trajectory tracking tests where the input frequency was varied. The

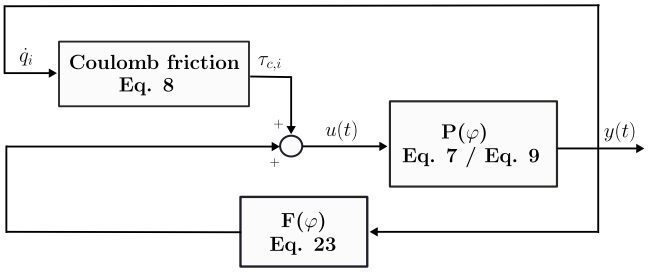

Figure 4. 2-DOF controller structure.

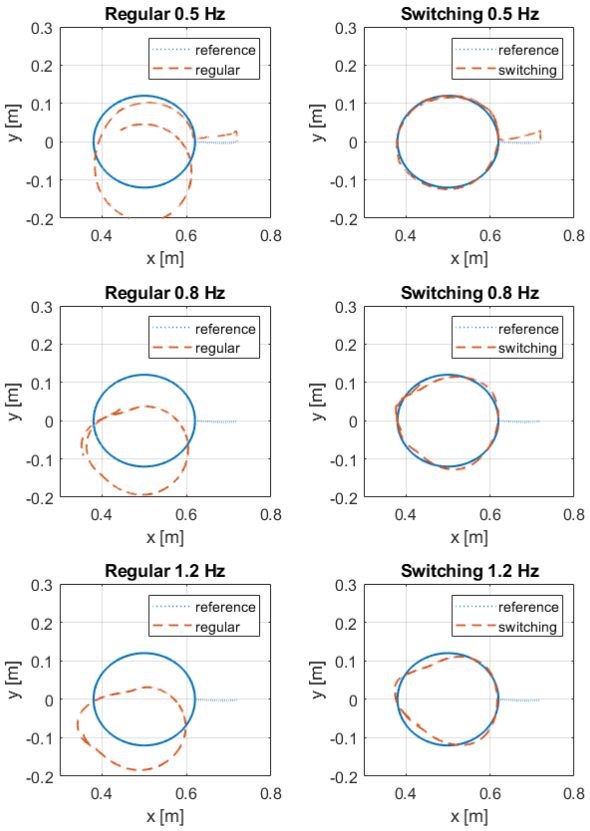

Figure 5. Reference tracking in case of circular TCP path with increasing frequency.

reference was defined for the tool centre point (TCP) of the robotic arm. It is obvious at first glance that the regular LPV solution struggles to keep steady tracking behaviour. When controller design conservatism was relaxed, a significant improvement could be reached.

Figure 6 and Figure 7 showcase the reference tracking quality for both the regular and switching LPV designs in time domain. It is worth noting that above the presented maximum frequency, the regular LPV cannot track the reference anymore and blows up. Another notable information to be gathered is that although nominal LPV is still a good choice in dynamic cases the major source of its inadequacy comes from the initial low dynamic – high reference error situation.

Figure 8 is a synthesis of the previous set of tests. Multiple frequencies were input to the robot in the form of a chirp. Obviously, even the better controller suffers some degradation moving towards the more dynamic parameter trajectory, but

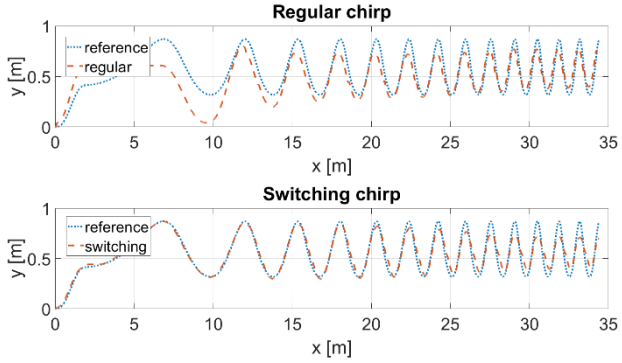

Figure 6. Angle reference tracking for arm 1 in time domain.

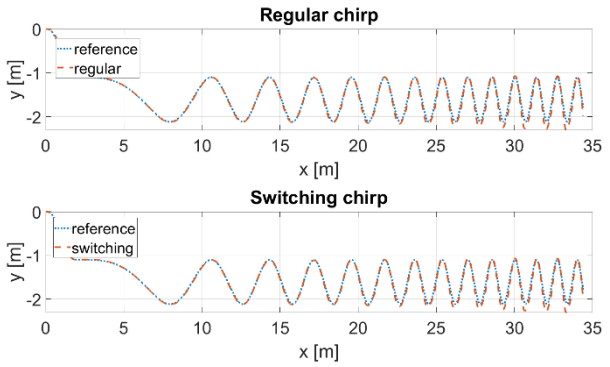

Figure 7. Angle reference tracking for arm 2 in time domain.

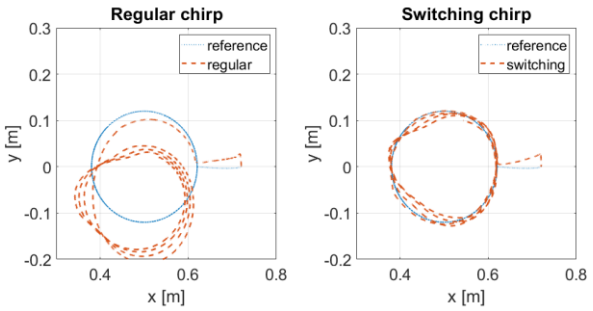

Figure 8. Reference tracking in case of circular TCP path with chirp input.

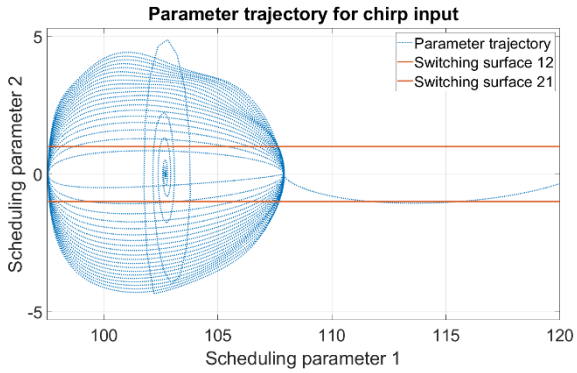

Figure 9. Parameter trajectories and controller switching during chirp.

degradation is not as severe and base performance is significantly better resulting in much better dynamic characteristics.

Figure 9 shows an example parameter trajectory for the chirp test case.

It is worth noting that no abrupt changes occur at any switching surfaces and the initial creeping phase happens almost entirely in the overlapping zone. Yet, performance in that range is what makes the difference between switching LPV and regular LPV.

P2P control was tested with step inputs on both arms presented in Figure 10 and Figure 11. In terms of dynamic tracking, the switching controller comes out as superior to the regular LPV. However, the more remarkable characteristic is the difference between steady-state errors. Both chirp input and step input results suggest that the major problem with the regular

[1] Absolute integral error was calculated with 0.002 s sampling time.

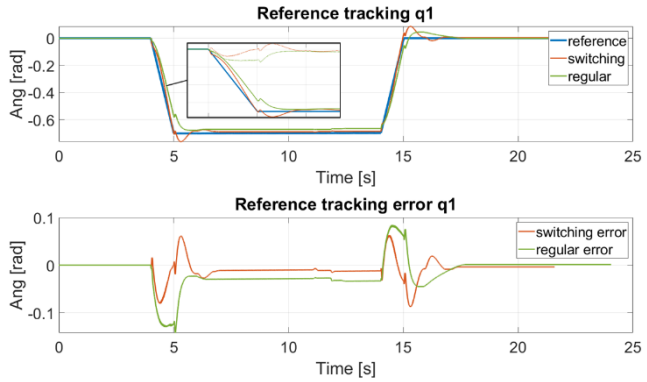

Figure 10. Angle reference tracking for arm 1 in case of step TCP path.

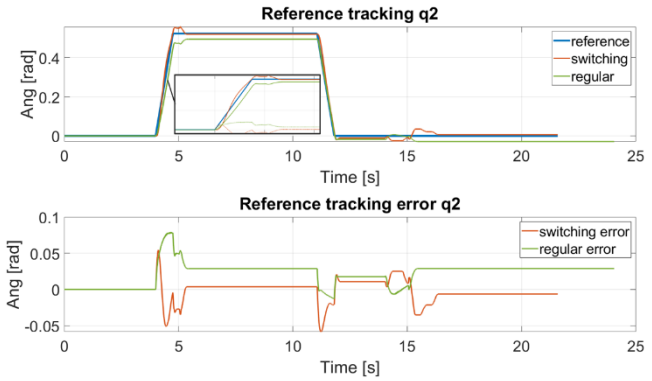

Figure 11. Angle reference tracking for arm 2 in case of step TCP path.

Table 2. Controller performance comparison.

Performance metric	Regular LPV	Switching LPV
Integral error 0.5 Hz (5 sec)[1]	1.23 m	0.21 m
Integral error 0.8 Hz (5 sec)	1.39 m	0.35 m
Integral error 1.2 Hz (5 sec)	1.41 m	0.51 m
Integral error chirp (0.2 – 1.5 Hz))	1.51 m	0.389 m
Lag at 0.7 of setpoint q_1[2]	0.08 s	0.31 s
Lag at 0.7 of setpoint q_2	NA	0.15 s
Steady state error q_1	0.009 rad	0.0026 rad
Steady state error q_2	0.04 rad	0.0037 rad

LPV occurs in low dynamic situations, consequently, in these cases the switching LPV rises above the traditional design.

Table 2 Presents an overview of the numerical results.

6. CONCLUSIONS

A switching LPV controller design study was presented for a 2-DOF robotic arm considering LMI-based H_∞ criterion. Selection of scheduling variables, variable sensitivity analysis, subdivision design and switching strategies were tested as design options. Results showed that switching LPV introduced a better performance by successfully reducing controller conservatism while maintaining every favourable characteristic of classical LPV controllers. Consequences on design strategies were drawn, and extensive controller performance measurement test series were run. The results indicated significant improvement in terms

[2] For safety reasons, the step experiment was conducted with a ramp rate and thus the usual delay time and rise time metrics do not apply.

of both dynamics and steady-state behaviour. As a future improvement possibility, the introduction of an adequate switching smoothness criterion is worthwhile, although in the case of the robot, chattering did not prove to be a significant issue. Moreover, a systematic approach to the design of subregion layouts is still lacking in the literature.

REFERENCES

[1] P. Gahinet, P. Apkarian, A linear matrix inequality approach to H∞ control, International Journal of Robust and Nonlinear Control, vol. 4 (1994), no. 4, pp. 421-448. DOI: 10.1002/rnc.4590040403

[2] P. Apkarian, P. Gahinet, G. Becker, Self-scheduled H∞ control of linear parameter-varying systems: a design example, Automatica, vol. 31 (1995), no. 9, pp. 1251-1261. DOI: 10.1016/0005-1098(95)00038-X

[3] C. W. Scherer, Multiobjective H2/H∞Control, IEEE Trans Automat Contr, vol. 40 (1995), no. 6, pp. 1054-1062. DOI: 10.1109/9.388682

[4] W. J. Rugh, J. S. Shamma, Research on gain scheduling, Automatica, vol. 36, issue 10, 2000, pp. 1401-1425. DOI: 10.1016/S0005-1098(00)00058-3

[5] Z. Yu, H. Chen, P. Y. Woo, Gain scheduled LPV H∞ control based on LMI approach for a robotic manipulator, J Robot Syst, vol. 19 (2002), no. 12, pp. 585-593. DOI: 10.1002/rob.10062

[6] S. M. Hashemi, H. S. Abbas, H. Werner, LPV modelling and control of a 2-DOF robotic manipulator using PCA-based parameter set mapping, Proc. of the IEEE Conf. on Decision and Control, Shanghai, China, 15-18 December 2009, pp. 7418-7423. DOI: 10.1109/CDC.2009.5400621

[7] S. Z. Rizvi, J. Mohammadpour, R. Toth, N. Meskin, A Kernel-Based PCA Approach to Model Reduction of Linear Parameter-Varying Systems, IEEE Transactions on Control Systems Technology, vol. 24 (2016), no. 5, pp. 1883-1891. DOI: 10.1109/TCST.2016.2517126

[8] A. San-Miguel, V. Puig, G. Alenyà, Disturbance observer-based LPV feedback control of a N-DoF robotic manipulator including compliance through gain shifting, Control Eng Pract, vol. 115 (2021), 104887. DOI: 10.1016/j.conengprac.2021.104887

[9] S. M. Hashemi, H. S. Abbas, H. Werner, Low-complexity linear parameter-varying modeling and control of a robotic manipulator, Control Eng Pract, vol. 20 (2012), no. 3, pp. 248-257. DOI: 10.1016/j.conengprac.2011.11.002

[10] P. Baranyi, TP model transformation as a way to LMI-based controller design, IEEE Transactions on Industrial Electronics, vol. 51 (2004), no. 2, pp. 387-400. DOI: 10.1109/TIE.2003.822037

[11] P. Gahinet, P. Apkarian, M. Chilali, Affine parameter-dependent Lyapunov functions and real parametric uncertainty, IEEE Trans Automat Contr, vol. 41 (1996), no. 3, pp. 436–442. DOI: 10.1109/9.486646

[12] S. Chumalee, J. F. Whidborne, Gain-scheduled H∞ control via parameter-dependent Lyapunov functions, Int J Syst Sci, vol. 46 (2015), no. 1, pp. 125–138. DOI: 10.1080/00207721.2013.775386

[13] B. Lu, F. Wu, Switching LPV control designs using multiple parameter-dependent Lyapunov functions, Automatica, vol. 40 (2004), no. 11, pp. 1973-1980. DOI: 10.1016/j.automatica.2004.06.011

[14] B. Lu, F. Wu, Control design of switched LPV systems using multiple parameter-dependent Lyapunov functions, Proc. of the American Control Conf., Boston, MA, USA, 30 June-2 July 2004, pp. 3875-3880. DOI: 10.23919/ACC.2004.1384517

[15] W. Jiang, C. Dong, Q. Wang, A systematic method of smooth switching LPV controllers design for a morphing aircraft, Chinese Journal of Aeronautics, vol. 28 (2015), no. 6, pp. 1640-1649. DOI: 10.1016/j.cja.2015.10.005

[16] B. Huang, B. Lu, Q. Li, Y. Tong, Average Dwell Time Based Smooth Switching Linear Parameter-Varying Proportional-Integral-Derivative Control for an F-16 Aircraft, IEEE Access, vol. 9 (2021), pp. 30979-30992. DOI: 10.1109/ACCESS.2021.3059900

[17] D. Yang, J. Zhao, H∞ output tracking control for a class of switched LPV systems and its application to an aero-engine model, International Journal of Robust and Nonlinear Control, vol. 27 (2017), no. 12, pp. 2102-2120. DOI: 10.1002/rnc.3673

[18] T. He, G. G. Zhu, S. S. M. Swei, W. Su, Smooth-switching LPV control for vibration suppression of a flexible airplane wing, Aerosp Sci Technol, vol. 84 (2019), pp. 895-903. DOI: 10.1016/j.ast.2018.11.029

[19] B. Lu, F. Wu, S. W. Kim, Switching LPV control of an F-16 aircraft via controller state reset, IEEE Transactions on Control Systems Technology, vol. 14 (2006), no. 2, pp. 267-277. DOI: 10.1109/TCST.2005.863656

[20] T. He, G. G. Zhu, S. S. M. Swei, A Sequential Design Approach for Switching $\mathfrak{H}$ ∞ LPV Control, Int J Control Autom Syst, vol. 19 (2021), no. 10, pp. 3354–3367. DOI: 10.1007/s12555-020-0363-3

[21] Z. Téczely, B. Kiss, Optimal Segmentation of LPV Systems for Control Applications via Genetic Algorithms, in Proceedings of the 21st Int. Conf. on Informatics in Control, Automation and Robotics - Volume 1: ICINCO, SciTePress, 2024, pp. 503–510. Online [Accessed 17 June 2025] https://www.scitepress.org/Papers/2024/130672/130672.pdf

[22] D. Szabó, E. G. Szádeczky-Kardoss, Dynamic parameter identification method for robotic arms with static friction modelling, Acta IMEKO, vol. 10 (2021), no. 3, pp. 44-50. DOI: 10.21014/ACTA_IMEKO.V10I3.1032

[23] H. Ohtake, K. Tanaka, H. O. Wang, Fuzzy modeling via sector nonlinearity concept, in Annual Conference of the North American Fuzzy Information Processing Society - NAFIPS, 2001, pp. 127-132. DOI: 10.1109/nafips.2001.944239

[24] P. Li, A. T. Nguyen, H. Du, Y. Wang, H. Zhang, Polytopic LPV approaches for intelligent automotive systems: State of the art and future challenges, 2021, 107931. DOI: 10.1016/j.ymssp.2021.107931

[25] V. A. Yakubovich, Linear Matrix Inequalities in System and Control Theory (S. Boyd, L. E. Ghaoui, E. Feron, and V. Balakrishnan), SIAM Review, vol. 37 (1995), no. 3, pp. . 479-481. DOI: 10.1137/1037119

[26] Z. Téczely, B. Kiss, LPV state-feedback control of a robotic manipulator via LMI optimization, XXIX Int. Conf. on Information, Communication and Automation Technologies (ICAT), Sarajevo, Bosnia and Herzegovina, 11-14 June 2023, pp. 1–6. DOI: 10.1109/ICAT57854.2023.10171295

[27] P. Gahinet, A. Nemirovskii, A. J. Laub, M. Chilali, The LMI control toolbox, Proc. of the 33rd IEEE Conf. on Decision and Control, Lake Buena Vista, FL, USA, 14-16 December 1994, vol.3, pp. 2038-2041. DOI: 10.1109/CDC.1994.411440

[28] B. Finta, B. Kiss, Two-Degree s-of-Freedom Controller Synthesis to Robustify the Computed Torque Method, 23rd IEEE Int. Symp. on Measurement and Control in Robotics, ISMCR 2020, 15-17 October 2020, pp. 1-6. DOI: 10.1109/ISMCR51255.2020.9263772